

RSMA-Enabled Covert Communications Against Multiple Spatially Random Wardens

Xinyue Pei, Jihao Liu, Xuewen Luo, Xingwei Wang, Yingyang Chen, *Senior Member, IEEE*,
Miaowen Wen, *Senior Member, IEEE*, and Theodoros A. Tsiftsis, *Senior Member, IEEE*

Abstract—This work investigates covert communication in a rate-splitting multiple access (RSMA)-based multi-user multiple-input single-output system, where the random locations of the wardens follow a homogeneous Poisson point process. To demonstrate practical deployment scenarios, imperfect channel state information at the transmitter is considered. Closed-form expressions for the statistics of the received signal-to-interference-plus-noise ratio, along with the analytical formulations for the covertness constraint, outage probability, and effective covert throughput (ECT), are derived. Subsequently, an ECT maximization problem is formulated under covertness and power allocation constraints. This optimization problem is addressed using an alternating optimization-assisted genetic algorithm (AO-GA). Simulation results corroborate the theoretical analysis and demonstrate the superiority of RSMA over conventional multiple access schemes, as well as the effectiveness of the proposed AO-GA.

Index Terms—Throughput, outage probability (OP), rate-splitting multiple access (RSMA), covert communications (CC), stochastic geometry.

I. INTRODUCTION

Rate-splitting multiple access (RSMA) has emerged as a promising technique for scenarios requiring robust and flexible interference management [1]. By integrating the rate splitting strategy at the transmitter with successive interference cancellation (SIC) at the receiver, RSMA outperforms space division multiple access (SDMA) and non-orthogonal multiple access (NOMA) in downlink multi-user multiple-input single-output (MU-MISO) scenarios [2].

However, the broadcast nature of wireless channels poses significant threats to the security of RSMA systems. Traditional techniques like cryptographic encryption and physical layer security have been employed to prevent information from being decoded by wardens [3]. Nevertheless, these methods cannot prevent communication activities from being monitored. In contrast, covert communication (CC) enhances both security and privacy by concealing the existence of transmissions from wardens [4].

X. Pei, J. Liu, X. Luo, and X. Wang are with School of Computer Science and Engineering, Northeastern University, Shenyang 110819, China (e-mail: peixy@cse.neu.edu.cn, 2310734@stu.neu.edu.cn, luoxw@cse.neu.edu.cn, wangxw@mail.neu.edu.cn).

Y. Chen is with the College of Information Science and Technology, Jinan University, Guangzhou 510632, China (e-mail: chenyy@jnu.edu.cn).

M. Wen is with the National Engineering Technology Research Center for Mobile Ultrasonic Detection, South China University of Technology, Guangzhou 510640, China (e-mail: eemwwen@scut.edu.cn).

T. A. Tsiftsis is with Department of Informatics Telecommunications, University of Thessaly, Lamia 35100, Greece, and also with the Department of Electrical and Electronic Engineering, University of Nottingham Ningbo China, Ningbo 315100, China (e-mail: tsiftsis@uth.gr).

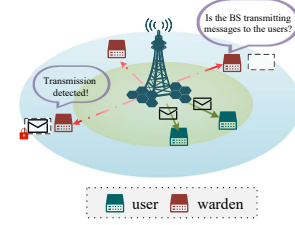


Fig. 1. The proposed system model. The green disc region represents the protected zone, and the blue annular region is the area where wardens are distributed.

Several works have studied the covertness of RSMA systems. Specifically, [5]–[9] investigated optimization strategies for enhancing CC performance in MISO RSMA systems. In parallel, [10]–[12] have conducted performance analyses of RSMA-based CC systems under various architectures, focusing on key metrics such as detection error probability (DEP), outage probability (OP), and covert transmission rate.

Notably, existing studies [5]–[12] primarily consider either a single warden or multiple static wardens. However, in practice, it is challenging for the base station (BS) to obtain accurate information about the number and locations of wardens, especially when they remain silent. Stochastic geometry provides a powerful analytical framework to model the spatial randomness of such unknown and silent wardens [13], [14]. To the best of the authors' knowledge, CC performance in RSMA systems with multiple randomly distributed wardens lacks in-depth investigation, which motivates us in this work.

In this work, we consider a MU-MISO RSMA-based CC system, where wardens are randomly distributed according to a homogeneous Poisson point process (HPPP). To ensure a realistic and practical scenario, imperfect channel state information at the transmitter (CSIT) is also taken into account. Our contributions can be summarized as follows:

- Closed-form cumulative distribution functions (CDFs) of received signal-to-interference-plus-noise ratios (SINRs) are derived and used to analyze the theoretical expressions for covertness constraint, OP, and effective covert throughput (ECT) under imperfect CSIT and randomly located wardens.
- An ECT maximization problem is formulated by jointly optimizing the transmit power and the common power coefficient. Due to the non-convex nature of the objective function and the intractability of its gradients, an alternating optimization-assisted genetic algorithm (AO-GA) is proposed.
- Monte Carlo simulations validate the accuracy of the

derived theoretical expressions and confirm that the proposed RSMA scheme outperforms NOMA and SDMA. Simulation results also verify the effectiveness of the proposed AO-GA.¹

II. SYSTEM MODEL

We consider a downlink RSMA-based CC system as shown in Fig. 1, where an M -antenna BS serves K single-antenna covert users, indexed by $k \in \mathcal{K} = \{1, \dots, K\}$, with $M \geq K$. Meanwhile, multiple non-colluding passive single-antenna wardens attempt to detect the covert transmission. These wardens, indexed by v , are spatially distributed according to a HPPP Φ_E with density λ_e , modeling their unknown random locations and numbers. It is assumed that wardens can be detected near the BS, and thus a protect zone, defined as a disc of radius r_p centered at the BS, is established.² To enhance covertness, covert users are assumed to be located within this zone. Outside this zone, wardens are spatially distributed over the infinite two-dimensional plane.

Without loss of generality, all channels are assumed to experience independent Rayleigh fading with large-scale path loss. The channel from BS to node ι ($\iota \in \{k, v\}$) is given by $\mathbf{h}_\iota = \sqrt{\beta_\iota} \mathbf{g}_\iota$ ($\mathbf{h}_\iota, \mathbf{g}_\iota \in \mathbb{C}^{M \times 1}$), where $\beta_\iota \triangleq d_\iota^{-\alpha}$ models the large-scale fading with α being the path loss exponent, and \mathbf{g}_ι is the small-scale fading vector with independent and identically distributed (i.i.d.) entries modeled as $\mathcal{CN}(0, 1)$. Notably, we consider a worst-case secrecy scenario, where the BS has imperfect CSIT of covert users and only statistical knowledge of the wardens' channels, lacking their instantaneous CSI [3], [16]. Then, the accurate channel vector from BS to U_k is expressed as $\mathbf{g}_k = \sqrt{\epsilon^2} \hat{\mathbf{g}}_k + \sqrt{1 - \epsilon^2} \Delta \mathbf{g}_k$, where $\hat{\mathbf{g}}_k$ and $\Delta \mathbf{g}_k$ respectively represent the estimated channel and estimation error, each consisting of i.i.d. $\mathcal{CN}(0, 1)$ entries. The parameter $\epsilon \in [0, 1]$ reflects the level of CSIT uncertainty with a smaller ϵ indicating worse CSIT quality.

Following RSMA protocol, each message intended for the k -th user (denoted by U_k) is divided into common and private parts. The common parts of all users are jointly encoded into a common stream s_c , while the private part of U_k is encoded into private stream s_k . It is assumed that $\mathbb{E}[|s_c|^2] = \mathbb{E}[|s_k|^2] = 1$, with corresponding power allocation coefficients a_c and a_k , satisfying $a_c + \sum_{k \in \mathcal{K}} a_k = 1$. Consequently, the signal transmitted by the BS can be derived as $\mathbf{s} = \sqrt{P a_c} \mathbf{w}_c s_c + \sum_{k=1}^K \sqrt{P a_k} \mathbf{w}_k s_k$, where P represents the total transmit power, while $\mathbf{w}_c, \mathbf{w}_k \in \mathbb{C}^{M \times 1}$ respectively denote the normalized precoders for the common and private streams.

¹Notation: The operations $\Pr(\cdot)$, $|\cdot|$, and $\mathbb{E}\{\cdot\}$ denote the probability, the absolute value, and the expectation, respectively. $F_X(\cdot)$ and $f_X(\cdot)$ respectively denote the CDF and probability density function (PDF) of a random variable (RV) X . $\mathcal{CN}(\mu, \beta)$ denotes a complex Gaussian distribution with mean μ and variance β . A gamma distribution with shape parameter D and scale parameter θ is represented by $\Gamma(D, \theta)$, whose PDF is $1/(\Gamma(D)\theta^D)x^{D-1}\exp(-x/\theta)$, and CDF is $\gamma(D, x/\theta)/\Gamma(D)$, which can be rewritten as $1 - \exp(-x/\theta) \sum_{i=0}^{D-1} 1/i!(x/\theta)^i$ with positive integer D . $[\cdot]$ finds the nearest integer. $W_{\nu, \frac{1}{2} + \nu}(z) = z^{-\nu} \exp(z/2) \int_z^\infty t^{2\nu} \exp(-t) dt$ is the Whittaker function defined in [15, (9.224)].

²The BS can create such zone using various detection methods, e.g., metal detectors and X-ray scanners, to identify and eliminate nearby suspicious devices before transmission [3].

TABLE I
SHAPE AND SCALE PARAMETERS FOR DIFFERENT RVs

RV	Shape parameter	Scale parameter
$\sum_{j \in \mathcal{K}} a_j \mathbf{g}_k^H \mathbf{w}_j ^2$	$D_{y,k} = \frac{(M-K+1)\epsilon^2 a_k + (1-\epsilon^2)}{(M-K+1)\epsilon^2 a_k^2 + \sum_{j \in \mathcal{K}} a_j^2 (1-\epsilon^2)^2}$	$\hat{\theta}_{y,k} = \frac{(M-K+1)\epsilon^2 a_k^2 + \sum_{j \in \mathcal{K}} a_j^2 (1-\epsilon^2)^2}{(M-K+1)\epsilon^2 a_k + (1-\epsilon^2)}$
$\sum_{j \in \mathcal{K}} a_j \mathbf{g}_v^H \mathbf{w}_j ^2$	$D_1 = \frac{(1-\epsilon^2)}{\sum_{j \in \mathcal{K}} a_j^2}$	$\hat{\theta}_1 = \frac{\sum_{j \in \mathcal{K}} a_j}{1-\epsilon^2}$
$\sum_{j \in \mathcal{K} \setminus k} a_j \mathbf{g}_k^H \mathbf{w}_j ^2$	$D_{\mathcal{L},k} = \frac{(1-\epsilon^2 - a_k)}{\sum_{j \in \mathcal{K} \setminus k} a_j^2}$	$\hat{\theta}_{\mathcal{L},k} = \frac{\sum_{j \in \mathcal{K} \setminus k} a_j}{1-\epsilon^2 - a_k}$
$ \mathbf{g}_v^H \mathbf{w}_k ^2$	$D_Z = \frac{(M-K+1)\epsilon^2 + (1-\epsilon^2)^2}{(M-K+1)\epsilon^2 + (1-\epsilon^2)}$	$\hat{\theta}_Z = \frac{(M-K+1)\epsilon^2 + (1-\epsilon^2)^2}{(M-K+1)\epsilon^2 + (1-\epsilon^2)}$

To eliminate inter-user interference, the private streams utilize zero-forcing beamforming (ZFBF), ensuring $|\hat{\mathbf{g}}_k^H \mathbf{w}_j|^2 = 0$. In contrast, the common stream adopts a random Gaussian beamformer \mathbf{w}_c that remains statistically independent of $\hat{\mathbf{g}}_k$, $\Delta \mathbf{g}_k$, and \mathbf{w}_k [1], [2].³

The received signal at U_k can be written as $y_k = \mathbf{h}_k^H \mathbf{s} + n_k$, where $n_k \sim \mathcal{CN}(0, \sigma^2)$ represents the additive white Gaussian noise (AWGN) at U_k . According to RSMA protocol, U_k first decodes the common stream s_c by treating all private streams as interference. Next, by applying SIC, U_k removes s_c from y_k . After successfully canceling s_c , U_k decodes its desired private stream s_k , treating the private streams of other users as interference. Therefore, the corresponding SINRs for decoding s_c and s_k at U_k are respectively given by

$$\gamma_{c,k} = \frac{\mathcal{P} a_c |\mathbf{h}_k^H \mathbf{w}_c|^2}{\sum_{j \in \mathcal{K}} \mathcal{P} a_j |\mathbf{h}_k^H \mathbf{w}_j|^2 + 1}, \quad \gamma_{p,k} = \frac{\mathcal{P} a_k |\mathbf{h}_k^H \mathbf{w}_k|^2}{\sum_{j \in \mathcal{K} \setminus k} \mathcal{P} a_j |\mathbf{h}_k^H \mathbf{w}_j|^2 + 1}, \quad (1)$$

where $\mathcal{P} = P/\sigma^2$ denotes the transmit signal-to-noise ratio (SNR) at BS.

Then, we focus on the detection process at the wardens. A typical v -th warden (denoted by warden- v) monitors the BS's activity and distinguishes between two hypotheses [13]:

$$\begin{cases} \mathcal{H}_0: & y_v = n_v, & (\text{BS is silent}) \\ \mathcal{H}_1: & y_v = \mathbf{h}_v^H \mathbf{s} + n_v, & (\text{BS is transmitting}) \end{cases} \quad (2)$$

where y_v and $n_v \sim \mathcal{CN}(0, \sigma^2)$ denote the received signal and the AWGN at warden- v , respectively.

Based on the above hypotheses, warden- v performs a binary hypothesis test. Let \mathcal{D}_0 and \mathcal{D}_1 denote the decisions favoring \mathcal{H}_0 and \mathcal{H}_1 , respectively. The reliability of this test is quantified by the total DEP, defined as [13]: $\xi_v = \mathbb{P}_{v,\text{FA}} + \mathbb{P}_{v,\text{MD}}$, where $\mathbb{P}_{v,\text{FA}} = \Pr(\mathcal{D}_1|\mathcal{H}_0)$ and $\mathbb{P}_{v,\text{MD}} = \Pr(\mathcal{D}_0|\mathcal{H}_1)$ denote the false alarm and the miss detection probabilities at warden- v , respectively. Under optimal detection, the warden minimizes the DEP to ξ_v^* . To guarantee CC, the system must satisfy $\xi_v^* \geq 1 - \varsigma$, where $\varsigma \in [0, 1]$ is a predefined covertness tolerance, ensuring that the warden's detection capability remains below an acceptable threshold. Under the non-colluding detection strategy, each warden independently determines whether the BS is transmitting signals based on its own observation. In this scenario, the CC performance of the system is dominated by the most detrimental warden with the minimal ξ_v^* . To ensure covertness, the system must guarantee $\xi_w = \min_{v \in \Phi_E} \{\xi_v^*\} \geq 1 - \varsigma$.

III. STATISTICAL ANALYSIS OF SINRS

To obtain the theoretical expressions of key performance metrics, we first investigate the statistics of received SINRs

³Employing ZFBF for the private streams and random precoding for the common stream is proven to be the optimal Degree of Freedom (DoF) in MISO broadcast channels scenarios with imperfect CSIT [2].

and obtain the following lemmas.

Lemma 1: The CDF of $\gamma_{c,k}$ can be derived as

$$F_{\gamma_{c,k}}(x) = 1 - \exp(-\varphi_k x)(\mu_k x + 1)^{-D_{\mathcal{Y},k}}, \quad (3)$$

where $\mu_k = \hat{\theta}_{\mathcal{Y},k}/a_c$, $\varphi_k = 1/(\mathcal{P}a_c\beta_k)$; $D_{\mathcal{Y},k}$ and $\hat{\theta}_{\mathcal{Y},k}$ have been defined in Table I.

Proof: See Appendix A. ■

Lemma 2: The CDF of $\gamma_{p,k}$ can be derived as

$$F_{\gamma_{p,k}}(x) = 1 - \sum_{m=0}^{\lfloor D_{\mathcal{Z}} \rfloor - 1} \sum_{n=0}^{\lfloor D_{\mathcal{Z}} \rfloor - m - 1} \frac{\exp\left(-\frac{x}{\theta_{\mathcal{Z}}}\right) x^{m+n} \psi_k}{(x\theta_{\mathcal{L},k} + \theta_{\mathcal{Z}})^{n+D_{\mathcal{L},k}}}, \quad (4)$$

where $\psi_k = \frac{\theta_{\mathcal{L},k}^n \theta_{\mathcal{Z}}^{D_{\mathcal{L},k}-m} \Gamma(n+D_{\mathcal{L},k})}{m!n!\Gamma(D_{\mathcal{L},k})}$, $\theta_{\mathcal{L},k} = \mathcal{P}\beta_k(1-\epsilon^2)\hat{\theta}_{\mathcal{L},k}$, and $\theta_{\mathcal{Z}} = \mathcal{P}a_k\beta_k\hat{\theta}_{\mathcal{Z}}$; $D_{\mathcal{L},k}$, $D_{\mathcal{Z}}$, $\hat{\theta}_{\mathcal{L},k}$, and $\hat{\theta}_{\mathcal{Z}}$ have been defined in Table I.

Proof: See Appendix B. ■

IV. PERFORMANCE ANALYSIS

In this section, we investigate the key metrics for CC performance of RSMA systems, including covertness constraint, OP, and the ECT.

A. Covertness Constraint

In this subsection, we aim to analyze the system's covertness by deriving the closed-form expression for the minimum DEP across all wardens, i.e., $\xi_w = \min_{v \in \Phi_E} \{\xi_v^*\} \geq 1 - \varsigma$. However, deriving ξ_v^* is analytically intractable, which complicates the analysis of ξ_w . To solve this challenge, we adopt Pinsker's inequality, yielding a lower bound for ξ_v^* [4], [8], [13], [14]:

$$\xi_v^* \geq 1 - \sqrt{\frac{1}{2} \mathcal{D}(p_1(y_v) \| p_0(y_v))}, \quad (5)$$

where $p_0(y_v)$ and $p_1(y_v)$ respectively denote the likelihood functions of the received signals of warden- v under \mathcal{H}_0 and \mathcal{H}_1 , and $\mathcal{D}(p_1 \| p_0)$ denotes the Kullback-Leibler (KL) divergence from $p_1(y_v)$ to $p_0(y_v)$. Then substituting (5) into $\xi_w \geq 1 - \varsigma$, the system covertness can be guaranteed by satisfying the equivalent condition: $\max_{v \in \Phi_E} \left\{ \sqrt{\frac{1}{2} \mathcal{D}(p_1(y_v) \| p_0(y_v))} \right\} \leq \varsigma$.

Recall that wardens are passive, and thus their instantaneous CSIs are unknown to the BS. Recall that only the statistical CSIs of the wardens are available. To this end, the average KL divergence is adopted in this work, where the expectation is taken over the spatial distribution and the small-scale fading statistics of wardens. Accordingly, the CC constraint for warden- v can be expressed as [13], [14]:

$$\mathbb{E} \left\{ \max_{v \in \Phi_E} \left\{ \sqrt{\frac{1}{2} \mathcal{D}(p_1(y_v) \| p_0(y_v))} \right\} \right\} \leq \varsigma. \quad (6)$$

Then we can achieve a tractable expression of covertness constraint in the following lemma:

Lemma 3: The expressions for covertness constraint considering HPPP distributed and non-colluding wardens can be derived as $\nu \mathcal{P} \leq \varsigma$, where

$$\nu = \frac{(\lambda_e \pi)^{\frac{\alpha}{4}} \exp\left(\frac{\lambda_e \pi r_p^2}{2}\right) W_{-\frac{\alpha}{4}, \frac{1}{2} - \frac{\alpha}{4}}(\lambda_e \pi r_p^2)}{2r_p^{\frac{\alpha}{2}}}. \quad (7)$$

Proof: See Appendix C. ■

Remark 1: It is observed that ν depends only on path loss exponent α , protected zone radius r_p , and warden density λ_e , regardless of the power allocation coefficients or the number of transmit antennas.

B. Outage Probability Analysis

Given that OP is crucial, we present its analysis below. Under RSMA protocol, an outage occurs at U_k when it fails to decode either s_c or s_k . Thus the OP of U_k can be expressed as

$$P_{\text{out},k} = \Pr(\gamma_{c,k} < \gamma_{k,th}^{s_c}) + \Pr(\gamma_{p,k} < \gamma_{k,th}^{s_k}) - \underbrace{\Pr(\gamma_{c,k} < \gamma_{k,th}^{s_c}, \gamma_{p,k} < \gamma_{k,th}^{s_k})}_{I_p}, \quad (8)$$

where $\gamma_{k,th}^{s_c}$ and $\gamma_{k,th}^{s_p}$ are the SINR thresholds of s_c and s_k at U_k , respectively. Specifically, the theoretical expression of $P_{\text{out},k}$ is summarized in the following lemma.

Lemma 4: The OP of U_k can be derived as

$$P_{\text{out},k} = \max \{F_{\gamma_{c,k}}(\gamma_{k,th}^{s_c}), F_{\gamma_{p,k}}(\gamma_{k,th}^{s_k})\}. \quad (9)$$

Proof: Due to the shared structure and the presence of Gamma-distributed terms, characterizing I_p becomes intractable. Following methods in [10]–[12], I_p can be tightly approximated as $\min\{F_{\gamma_{c,k}}(\gamma_{k,th}^{s_c}), F_{\gamma_{p,k}}(\gamma_{k,th}^{s_k})\}$, which enables a tractable expression of $P_{\text{out},k}$. ■

C. Effective Covert Throughput Analysis

This subsection focuses on maximizing the ECT, which is defined as the achievable effective throughput under the covertness constraint [13], [14]. Based on the decoding order of s_c and s_k , the effective throughput of U_k is given by [2], [17]:

$$\tau_k = R_{c,k} \Pr(\gamma_{c,k} \geq \gamma_{k,th}^{s_c}) + R_{p,k} (1 - P_{\text{out},k}), \quad (10)$$

where $R_{c,k} = \log_2(1 + \gamma_{k,th}^{s_c})$ and $R_{p,k} = \log_2(1 + \gamma_{k,th}^{s_k})$ denote the target rates of s_c and s_k , respectively. To maximize ECT, we optimize the transmit SNR \mathcal{P} and the power allocation coefficient a_c . For tractability, we assume $a_k = (1 - a_c)/K$, which is reasonable for symmetric users with identical channel statistics [1]. Then the optimization problem can be formulated as

$$\mathbf{P}_0 : \max_{\mathcal{P}, a_c} \tau \text{ s.t. } \nu \mathcal{P} \leq \varsigma, a_c \in [0, 1], \mathcal{P} > 0. \quad (11)$$

However, from Eqs. (3), (4), and (9), it is evident that τ is a highly complex and non-convex function with respect to both \mathcal{P} and a_c . The lack of analytical gradients and unclear monotonicity further hinder the use of conventional convex optimization or gradient-based methods. To address this, we first adopt the AO approach to decompose \mathbf{P}_0 into two simpler sub-problems:

$$\mathbf{P}_1 : \max_{\mathcal{P}} \tau \text{ s.t. } \mathcal{P} \in (0, \varsigma/\nu], \quad \mathbf{P}_2 : \max_{a_c} \tau \text{ s.t. } a_c \in [0, 1]. \quad (12)$$

Unfortunately, both \mathbf{P}_1 and \mathbf{P}_2 inherit the non-convexity and gradient intractability of \mathbf{P}_0 . Therefore, we resort to the GA to efficiently solve these subproblems. The overall optimization procedure is summarized in Algorithm 1.

Remark 2: The overall computational complexity of Algorithm 1 is $\mathcal{O}(I_{\text{AO}}(\sum_{i=1}^2 N_{g,i}(N_{p,i} - N_{e,i})[D_{\mathcal{Z}}]^2 K))$, where I_{AO} is the number of AO iterations, and the GA complexity for each \mathbf{P}_i depends on population size $N_{p,i}$, elitism size $N_{e,i}$, generations $N_{g,i}$, and fitness function $-\tau$.

V. NUMERICAL RESULTS

In this section, we verify the accuracy of theoretical expressions through Monte Carlo methods. Unless otherwise stated,

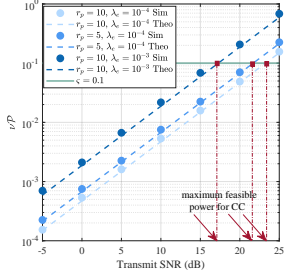


Fig. 2. Covertness constraint versus transmit SNR \mathcal{P} with different r_p and λ_e .

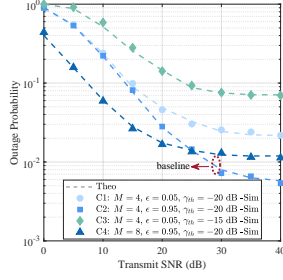


Fig. 3. OP versus transmit SNR \mathcal{P} with different Cases (denoted by C1-C4).

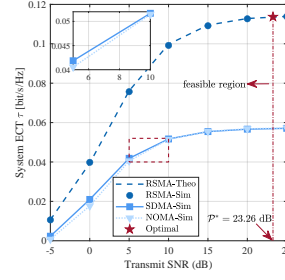


Fig. 4. System ECT versus transmit SNR \mathcal{P} .

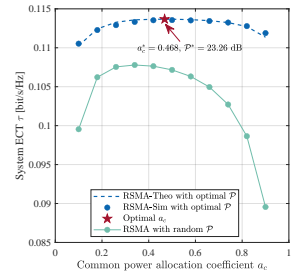


Fig. 5. System ECT versus common power allocation coefficient a_c .

Algorithm 1: AO-GA

Input: System parameters; tolerance e ; max iterations \mathcal{N}_{\max} .
Output: Optimized a_c^* and \mathcal{P}^* .

- 1 Randomly initialize $a_c^{(0)} \in [0, 1]$ and $\mathcal{P}^{(0)} \in (0, \varsigma/\nu]$, set iteration index $n = 0$;
- 2 **repeat**
- 3 Fix $a_c^{(n)}$, solve \mathbf{P}_1 using GA, obtain $\mathcal{P}^{(n+1)}$;
- 4 Fix $\mathcal{P}^{(n+1)}$, solve \mathbf{P}_2 using GA, obtain $a_c^{(n+1)}$;
- 5 **if** $|\tau^{(n+1)} - \tau^{(n)}| < e$ **then**
- 6 **break**;
- 7 **end**
- 8 $n \leftarrow n + 1$;
- 9 **until** convergence or $n > \mathcal{N}_{\max}$;
- 10 $a_c^* \leftarrow a_c^{(n)}$, $\mathcal{P}^* \leftarrow \mathcal{P}^{(n)}$;

the simulation parameters are set as follows [1], [11], [13], [14], [16]: $M = 4$, $K = 4$; $\epsilon = 0.95$; $a_c = 0.5$ and $a_k = (1 - a_c)/K$; $\alpha = 2$, $d_k = 5$ m, $r_p = 10$ m; $\varsigma = 0.1$; $\gamma_{k,th}^{sc} = \gamma_{k,th}^{sk} = \gamma_{th} = -20$ dB; $e = 10^{-9}$ and $\mathcal{N}_{\max} = 10$.

In Fig. 2, we plot the covertness constraint versus transmit SNR for different values of the radius of protected zone r_p and the density of warden distribution λ_e . It can be observed that $\nu\mathcal{P}$ is a monotonically increasing function of \mathcal{P} . As such, increasing λ_e enhances the multi-user diversity gain when selecting the most detrimental warden, while decreasing r_p strengthens the eavesdropping channel. Both operations lead to an increase in ν , thereby reducing the maximum feasible transmit power that satisfies the covertness constraint.

In Fig. 3, we compare the outage performance under four cases: C1 increases CSIT uncertainty; C2 adopts the baseline settings; C3 further raises the SINR threshold on top of C1; C4 increases the number of transmit antennas. Results show that higher channel uncertainty and SINR thresholds degrade outage performance. Notably, the 8-antenna RSMA system only outperforms its 4-antenna counterpart at low-to-medium SNR. Despite offering more spatial DoF, the 8-antenna scheme is more sensitive to CSIT uncertainty. At high SNR, even small estimation errors can cause beam misalignment and offset the benefits of high-dimensional precoding.

Fig. 4 shows the system ECT versus \mathcal{P} with the optimal $a_c^* = 0.468$ obtained via AO-GA. We compare the performance of the proposed RSMA scheme with that of SDMA using ZFBF (by setting $a_c = 0$), and NOMA with a random precoder, where a_k is determined through exhaustive search.

Clearly, RSMA outperforms both SDMA and NOMA, owing to its robustness and its ability to achieve the optimal DoF. In addition, it is observed that NOMA slightly performs worse than SDMA, as it can suffer from a loss of sum DoF due to the inefficient utilization of SIC when $M \geq K$. Furthermore, the effectiveness of AO-GA is verified in Fig. 5, where the optimal point is found at $\mathcal{P}^* = 23.26$ dB and $a_c^* = 0.468$.

VI. CONCLUSIONS

In this work, we have investigated a RSMA-based MU-MISO system consisting of a multi-antenna BS, several users, and multiple non-colluding HPPP-distributed wardens. Considering imperfect CSIT, we have derived theoretical expressions for the covertness constraint, OP, and ECT. Moreover, we have proposed the AO-GA to solve the system ECT optimization problem by jointly optimizing the transmit SNR and the common power allocation coefficient. The theoretical findings and the effectiveness of the AO-GA have been validated through simulation results. We have also explored the impacts of transmit SNR, HPPP density, CSIT uncertainty, protected zone radius, and SINR thresholds. Finally, simulation results have demonstrated that the proposed RSMA scheme can effectively mitigate the impact of CSIT uncertainty and exhibits superior covert performance against spatially random wardens compared to SDMA and NOMA.

APPENDIX A PROOF OF LEMMA 1

For convenience, define $\mathcal{X} = \mathcal{P}a_c\beta_k|\mathbf{g}_k^H\mathbf{w}_c|^2$ and $\mathcal{Y} = \sum_{j \in \mathcal{K}} \mathcal{P}a_j\beta_k|\mathbf{g}_k^H\mathbf{w}_j|^2$. Since \mathbf{w}_c is isotropically distributed and independent of \mathbf{g}_k , $\mathcal{X} \sim \Gamma(1, \mathcal{P}a_c\beta_k)$ [1]. To characterize the distribution of \mathcal{Y} , we first decompose the imperfect channel as $\mathbf{g}_k = \sqrt{\epsilon^2}\hat{\mathbf{g}}_k + \sqrt{1-\epsilon^2}\Delta\mathbf{g}_k$. For tractability, we ignore the cross-terms involving both $\hat{\mathbf{g}}_k$ and $\Delta\mathbf{g}_k$. Therefore, we have the following approximations:

$$a_k\beta_k|\mathbf{g}_k^H\mathbf{w}_k|^2 \approx a_k\beta_k \left(\epsilon^2|\hat{\mathbf{g}}_k^H\mathbf{w}_k|^2 + (1-\epsilon^2)|\Delta\mathbf{g}_k^H\mathbf{w}_k|^2 \right), \quad (\text{A.1a})$$

$$a_j\beta_k|\mathbf{g}_k^H\mathbf{w}_j|^2 \approx a_j\beta_k(1-\epsilon^2)|\Delta\mathbf{g}_k^H\mathbf{w}_j|^2. \quad (\text{A.1b})$$

Since \mathbf{w}_k is isotropic and independent of $\Delta\mathbf{g}_k$, we have $a_j(1-\epsilon^2)|\Delta\mathbf{g}_k^H\mathbf{w}_j|^2 \sim \Gamma(1, a_j(1-\epsilon^2))$ and $a_k(1-\epsilon^2)|\Delta\mathbf{g}_k^H\mathbf{w}_k|^2 \sim \Gamma(1, a_k(1-\epsilon^2))$. Furthermore, $a_k\epsilon^2|\hat{\mathbf{g}}_k^H\mathbf{w}_k|^2 \sim \Gamma(M-K+1, a_k\epsilon^2)$ [18].

By using moment-matching method in [18], the sum $\sum_{j \in \mathcal{K}} \Gamma(D_j, \theta_j)$ is approximated by $\Gamma(D, \theta)$, where $D =$

$\frac{(\sum_j D_j \theta_j)^2}{\sum_j D_j \theta_j^2}$ and $\theta = \frac{\sum_j D_j \theta_j^2}{\sum_j D_j \theta_j}$. Accordingly, we approximate $\mathcal{Y} \sim \Gamma(D_{\mathcal{Y},k}, \hat{\theta}_{\mathcal{Y},k} \mathcal{P} \beta_k)$, and then derive the CDF of $\gamma_{c,k}$ as

$$F_{\gamma_{c,k}}(x) = 1 - \frac{\exp\left(-\frac{x}{\mathcal{P} a_c \beta_k}\right)}{\theta_{\mathcal{Y},k}^{D_{\mathcal{Y},k}} \Gamma(D_{\mathcal{Y},k})} \int_0^\infty \exp(-I_0 y) y^{D_{\mathcal{Y},k}-1} dy, \quad (\text{A.2})$$

where $I_0 = \frac{x}{\mathcal{P} a_c \beta_k} + \frac{1}{\theta_{\mathcal{Y},k}}$. Using [15, Eq. (3.351.3)], (A.2) can be rewritten as (3), completing the proof.

APPENDIX B

PROOF OF LEMMA 2

Let $\mathcal{L} = \sum_{k \in \mathcal{K}} \mathcal{P} a_j \beta_k |\mathbf{g}_k^H \mathbf{w}_j|^2$ and $\mathcal{Z} = \mathcal{P} a_k \beta_k |\mathbf{g}_k^H \mathbf{w}_k|^2$. Following the moment-matching method in Appendix A, the distributions of \mathcal{L} and \mathcal{Z} can be approximated by $\Gamma(D_{\mathcal{L},k}, \theta_{\mathcal{L},k})$ and $\Gamma(D_{\mathcal{Z}}, \theta_{\mathcal{Z}})$, respectively. Accordingly, the CDF of $\gamma_{p,k}$ is given by

$$F_{\gamma_{p,k}}(x) = \int_0^\infty \underbrace{\frac{\gamma \left(D_{\mathcal{Z}}, \frac{x(l+1)}{\theta_{\mathcal{Z}}}\right)}{\Gamma(D_{\mathcal{Z}})}}_{I_1} \frac{l^{D_{\mathcal{L}}-1} \exp\left(-\frac{l}{\theta_{\mathcal{L}}}\right)}{\Gamma(D_{\mathcal{L}}) \theta_{\mathcal{L}}^{D_{\mathcal{L}}}} dl. \quad (\text{B.3})$$

Since the closed-form expression for the above integral is not available, we approximate $D_{\mathcal{Z}}$ by $\lfloor D_{\mathcal{Z}} \rfloor$. Then I_1 can be rewritten as

$$\begin{aligned} I_1 &\stackrel{(a)}{=} 1 - \exp\left(-\frac{x(l+1)}{\theta_{\mathcal{Z}}}\right) \sum_{m=0}^{\lfloor D_{\mathcal{Z}} \rfloor - 1} \sum_{k=m}^{\lfloor D_{\mathcal{Z}} \rfloor - 1} \binom{k}{m} \frac{1}{k!} \left(\frac{x}{\theta_{\mathcal{Z}}}\right)^k l^{k-m} \\ &\stackrel{(b)}{=} 1 - \sum_{m=0}^{\lfloor D_{\mathcal{Z}} \rfloor - 1} \sum_{n=0}^{\lfloor D_{\mathcal{Z}} \rfloor - m - 1} \kappa \exp\left(-\frac{x}{\theta_{\mathcal{Z}}} l\right) l^n, \end{aligned} \quad (\text{B.4})$$

where (a) is derived based on the CDF of $\Gamma(\lfloor D_{\mathcal{Z}} \rfloor, \theta_{\mathcal{Z}})$ and the binomial expansion, and (b) stands for $n = k - m$ and $\kappa = \frac{\exp\left(-\frac{x}{\theta_{\mathcal{Z}}}\right) \left(\frac{x}{\theta_{\mathcal{Z}}}\right)^{m+n}}{m!n!}$. Substituting (B.4) into (B.3) and applying [15, Eq. (3.326.2)], we finally arrive at (4).

APPENDIX C

PROOF OF LEMMA 3

Before deriving the closed-form expression for the covert-ness constraint, we first characterize the probability distribution of y_v . According to (2), the likelihood functions of y_v under hypotheses \mathcal{H}_0 and \mathcal{H}_1 are given by $p_0(y_v) = \exp(-|y_v|^2/\lambda_0)/(\pi\lambda_0)$ and $p_1(y_v) = \exp(-|y_v|^2/\lambda_1)/(\pi\lambda_1)$, where $\lambda_0 = \sigma^2$ and $\lambda_1 = \mathcal{P} a_c |\mathbf{h}_v^H \mathbf{w}_c|^2 + \sum_{k=1}^K \mathcal{P} a_k |\mathbf{h}_v^H \mathbf{w}_k|^2 + \sigma^2$. Then the KL divergence is given by [4, (11b)]:

$$\mathcal{D}(p_1(y_v)||p_0(y_v)) = \int_{-\infty}^{+\infty} p_1(y_v) \ln \frac{p_1(y_v)}{p_0(y_v)} dy_v = m - \ln(1+m), \quad (\text{C.1})$$

where $m = \frac{\lambda_1 - \lambda_0}{\lambda_0} = \mathcal{P} d_v^{-\alpha} \mathcal{M}$ and $\mathcal{M} = a_c |\mathbf{g}_v^H \mathbf{w}_c|^2 + \sum_{j \in \mathcal{K}} a_j |\mathbf{g}_v^H \mathbf{w}_j|^2$. Since \mathbf{w}_c and \mathbf{w}_j are isotropically distributed and independent of \mathbf{g}_v , RVs $a_c |\mathbf{g}_v^H \mathbf{w}_c|^2$ and $\sum_{j \in \mathcal{K}} a_j |\mathbf{g}_v^H \mathbf{w}_j|^2$ respectively follow $\Gamma(1, a_c)$ and $\Gamma(D_1, \hat{\theta}_1)$. As a result, \mathcal{M} can be approximated by $\Gamma(D_{\mathcal{M}}, \theta_{\mathcal{M}})$, where $D_{\mathcal{M}} = \frac{(a_c + D_1 \hat{\theta}_1)^2}{a_c^2 + D_1 \hat{\theta}_1^2}$ and $\theta_{\mathcal{M}} = \frac{a_c + D_1 \hat{\theta}_1}{a_c + D_1 \hat{\theta}_1}$.

Using the inequality $\ln(1+x) \geq x - x^2/2$ for $x > 0$, we obtain an upper bound for (C.1), i.e., $\mathcal{D}(p_1(y_v)||p_0(y_v)) \leq m^2/2$. Substituting this bound into (6), we arrive at $\zeta = \max_{v \in \Phi_E} \mathbb{E}_{\Phi_E} \{d_v^{-\alpha}\} \mathcal{P} m_0/2 \leq \varsigma$, where $m_0 = D_{\mathcal{M}} \theta_{\mathcal{M}} = 1$ is the mean of RV \mathcal{M} . In the following, we show how to evaluate ζ .

$$\zeta = \frac{\mathcal{P} m_0}{2} \int_{r_p}^\infty r^{-\alpha} f_{d_v}(r) dr$$

$$\begin{aligned} &\stackrel{(a)}{=} \frac{\mathcal{P} m_0 \lambda_e \pi}{\exp(-\lambda_e \pi r_p^2)} \int_{r_p}^\infty r^{1-\alpha} \exp(-\lambda_e \pi r^2) dr \\ &\stackrel{(b)}{=} \frac{\mathcal{P} m_0 (\lambda_e \pi)^{\alpha/2}}{2 \exp(-\lambda_e \pi r_p^2)} \int_{\pi \lambda_e r_p^2}^\infty \frac{\exp(-z)}{z^{\frac{\alpha}{2}}} dz, \end{aligned} \quad (\text{C.2})$$

where (a) can be arrived by using void probability over a HPPP [19]; (b) comes from $z = \lambda_e \pi r_p^2$. Finally, by applying [15, Eq. (3.381.6)], we arrive at $\nu \mathcal{P} \leq \varsigma$.

REFERENCES

- [1] O. Dizdar, Y. Mao, and B. Clerckx, "Rate-splitting multiple access to mitigate the curse of mobility in (massive) MIMO networks," *IEEE Trans. Commun.*, vol. 69, no. 10, pp. 6765–6780, 2021.
- [2] Y. Mao, O. Dizdar, B. Clerckx, R. Schober, P. Popovski, and H. V. Poor, "Rate-splitting multiple access: Fundamentals, survey, and future research trends," *IEEE Commun. Surveys Tuts.*, vol. 24, no. 4, pp. 2073–2126, 2022.
- [3] Y. Liu, Z. Qin, M. El-kashlan, Y. Gao, and L. Hanzo, "Enhancing the physical layer security of non-orthogonal multiple access in large-scale networks," *IEEE Trans. Wireless Commun.*, vol. 16, no. 3, pp. 1656–1672, 2017.
- [4] S. Ma, Y. Zhang, H. Li, S. Lu, N. Al-Dhahir, S. Zhang, and S. Li, "Robust beamforming design for covert communications," *IEEE Trans. Inf. Forensics Security*, vol. 16, pp. 3026–3038, 2021.
- [5] N. Q. Hieu, D. T. Hoang, D. Niyato, D. N. Nguyen, D. I. Kim, and A. Jamalipour, "Joint power allocation and rate control for rate splitting multiple access networks with covert communications," *IEEE Trans. Commun.*, vol. 71, no. 4, pp. 2274–2287, 2023.
- [6] T. T. Nguyen, N. C. Luong, S. Feng, K. Elbassioni, and D. Niyato, "Jamming-based covert communication for rate-splitting multiple access," *IEEE Trans. Veh. Technol.*, vol. 72, no. 8, pp. 11074–11079, 2023.
- [7] H. Chang, X. Kang, H. Lei, T. A. Tsiftsis, G. Pan, and H. Liu, "STAR-RIS-aided covert communications in MISO-RSMA systems," *IEEE Trans. Green Commun. Netw.*, vol. 8, no. 4, pp. 1318–1331, 2024.
- [8] Y. Zhang, W. Ni, Y. Mao, B. Ning, S. Xiao, W. Tang, and D. Niyato, "Rate-splitting multiple access for covert communications," *IEEE Wireless Commun. Lett.*, vol. 13, no. 6, pp. 1685–1689, 2024.
- [9] H. Jia, Y. Wang, W. Wu, and J. Yuan, "Robust transmission design for covert satellite communication systems with dual-CSI uncertainty," *IEEE Internet Things J.*, early access, 2025.
- [10] Y. Zhang, L. Yang, X. Li, K. Guo, and H. Liu, "Covert communications for STAR-RIS-assisted industrial networks with a full duplex receiver and RSMA," *IEEE Internet Things J.*, vol. 11, no. 12, pp. 22483–22493, 2024.
- [11] Z. Zhang, L. Yang, H. Lei, X. Li, and D. Niyato, "Covert communication in RSMA-assisted ambient backscatter communication systems," *IEEE Trans. Wireless Commun.*, early access, 2025.
- [12] Y. Liang, K. Huang, L. Yang, X. Li, H. Liu, and Y. Bian, "Covert communications for active STAR-RIS-aided RSMA systems with hardware impairments," *IEEE Trans. Intell. Transp. Syst.*, early access, 2025.
- [13] R. Ma, W. Yang, L. Tao, X. Lu, Z. Xiang, and J. Liu, "Covert communications with randomly distributed wardens in the finite blocklength regime," *IEEE Trans. Veh. Technol.*, vol. 71, no. 1, pp. 533–544, 2021.
- [14] R. Ma, W. Yang, X. Guan, X. Lu, Y. Song, and D. Chen, "Covert mmwave communications with finite blocklength against spatially random wardens," *IEEE Internet Things J.*, vol. 11, no. 2, pp. 3402–3416, 2023.
- [15] I. S. Gradshteyn and I. M. Ryzhik, *Table of integrals, series, and products*. Academic press, 2007.
- [16] X. Pei, Y. Chen, M. Wen, T. Pei, X. Wang, and T. A. Tsiftsis, "Secrecy performance analysis of RSMA-based communications under partial CSIT against randomly located eavesdroppers," *IEEE Trans. Veh. Technol.*, 2024.
- [17] T.-H. Vu, Q.-V. Pham, and S. Kim, "On performance of downlink THz-based rate-splitting multiple-access (RSMA): Is it always better than NOMA?" *IEEE Trans. Veh. Technol.*, vol. 73, no. 3, pp. 4435–4440, 2023.
- [18] D. Jaramillo-Ramirez, M. Kountouris, and E. Hardouin, "Coordinated multi-point transmission with imperfect CSI and other-cell interference," *IEEE Trans. Wireless Commun.*, vol. 14, no. 4, pp. 1882–1896, 2014.
- [19] M. Haenggi, *Stochastic geometry for wireless networks*. Cambridge University Press, 2013.